Bonding Geometry of Pyrrolyl in Zirconium Complexes: Fluxionality between σ and π Coordination

Alberto R. Dias, André P. Ferreira, and Luis F. Veiros*

Centro de Química Estrutural, Complexo I, Instituto Superior Técnico, Avenida Rovisco Pais 1, 1049-001 Lisbon, Portugal

Received July 9, 2003

The bonding geometry of pyrrolyl ligands (pyr′) in zirconium complexes was studied by means of DFT/B3LYP calculations with a DZVP basis set. Monopyrrolyl complexes, [Zr(pyr′)L_3], and bispyrrolyl species, [Zr(pyr′)$_2L_2$], were addressed, with different pyrrolyl ligands, pyr′ = pyrrolyl (pyr), 2,5-dimethylpyrrolyl (dmp), 2,4-dimethyl-3-ethylpyrrolyl (dmep), and ancillary ligands, L = chloride, methyl. Two coordination modes of pyr′ were considered. The first is the π coordination of pyr′, with the bonding to the metal established by means of the ring π orbitals. Slightly distorted η^5 coordination results, with the nitrogen tending to approach the metal. The second corresponds to a σ-pyr′, with the nitrogen lone pair used to establish a σ bond to the metal. The slippage from a π to a σ-pyr′ produces an electronically poorer metal center and results, normally, in a less stable complex, although this effect is partially compensated by a strengthening of the Zr−N in the σ coordination mode, when compared with the one existing in a π-pyr′. The σ-pyr′ coordination and the π-σ slippage were found to be disfavored by substituents in the α carbon atoms of pyr′, confirming a known empirical rule. The interconversion between the two coordination modes of the pyr′ ligand was studied in all the complexes and determined to correspond to a slippage process without any significant ring folding. In the corresponding transition states the Zr−C bond breaking process is completed for the two β carbon atoms, and the slipping pyr′ ring coordinates in a flat η^3 mode. The activation energies calculated for the slippage process in the various species (<10 kcal mol^{-1}) suggest the possibility of fluxionality in solution, even at room temperature. The mechanism for the *rac*/*meso* isomerization of [Zr(π-dmep)$_2$(CH_3)$_2$] was also studied and determined to proceed via consecutive slippage and rotation of the dmep ring, the rate-determining step corresponding to the first slippage of that ligand. The calculated activation energy (E_a < 7 kcal mol^{-1}) corroborates the experimental observation of fluxionality in solution, at room temperature.

Introduction

The cyclopentadienyl ligand (Cp = $C_5H_5^-$) plays a very important role in the organometallic chemistry of transition elements. In fact, complexes with cyclopentadienyl or with related, substituted derivatives of this ligand (Cp′) constitute a well-known domain of organometallic chemistry,[1] with relevant applications in areas as different as catalysis[2] and cancer therapy.[3,4] By comparison with Cp, the isoelectronic pyrrolyl ligand (pyr = $NC_4H_4^-$) or substituted pyrrolyls (pyr′) have been much less studied with respect to their reactions with transition metals[5−7] due not only to the historical relevance of the Cp ligand but also to the instability of the pyrrolyl metal complexes.

Scheme 1

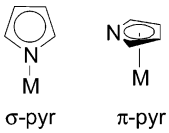

A search on the Cambridge Structural Database (CSD)[8] reveals that in most pyrrolyl transition metal complexes with a full structural characterization, that is, with determined X-ray structure, the pyrrolyl ligand coordinates in a N-σ mode, with the nitrogen lone pair establishing the pyr−metal bond (see Scheme 1). The alternative π coordination, with the entire π system of the pyrrolyl ligand involved in the bond, is comparatively rarer. In this case, a pentahapto (η^5) pyr results, although it is normally associated with some degree of slippage of the pyrrolyl ring, as the nitrogen atom tends to be closer to the metal, in what may be described as an intermediate coordination between η^5 and η^3.[9] The zirconium chemistry is no exception. In fact, the first

* Corresponding author. E-mail: veiros@ist.utl.pt. Phone: +351-218 419 283, Fax: +351-218 464 457.

(1) Crabtree, R. H. *The Organometallic Chemistry of the Transition Metals*, 3rd ed.; John Wiley and Sons: New York, 2001; p 129.
(2) Bochmann, M. *J. Chem. Soc., Dalton Trans.* **1996**, 255.
(3) Klapotke, T. M.; Kopt, H.; Tornieporth-Oetting, I. C.; White, P. S. *Organometallics* **1994**, *13*, 3268.
(4) Kupt-Maier, P. *Complexes in Cancer Chemotherapy*; Keppler, B. K., Ed.; VCH: New York, 1993; p 259.
(5) King, R. B.; Bisnette, M. B. *Inorg. Chem.* **1964**, *3*, 796.
(6) Kershner, D. L.; Basolo, F. *Coord. Chem. Rev.* **1987**, *75*, 279.
(7) Nief, F. *Eur. J. Inorg. Chem.* **2001**, 891.
(8) Allen, F. H. *Acta Crystallogr.* **2002**, *B58*, 380.
(9) Dias, A. R.; Galvão, A. M.; Galvão, A. C.; Salema, M. S. *J. Chem. Soc., Dalton Trans.* **1997**, 1055.

10.1021/om034029y CCC: $25.00
Publication on Web 10/29/2003

Scheme 2

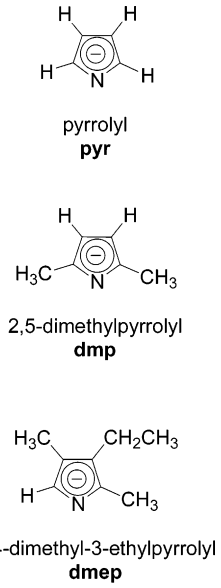

series of Zr complexes with η^5-pyr has been reported only very recently.[10]

The interconversion between π and σ coordination was observed in a *meso*-octaethylporphyrinogen Zr^{IV} complex, based on ^1H NMR results,[11] and pointed as the probable mechanism for the *rac*/*meso* isomerization of group 4 metal complexes with asymmetric phospholyl ligands ($PC_4PhMe_2H^-$).[12,13] However, a detailed study of the mechanism for the interconversion between the two coordination modes of heterocyclic ligands, such as pyrrolyl and phospholyl, has never been published, to the best of our knowledge. In the course of our studies of pyrrolyl transition metal chemistry,[9,14−16] recent NMR results were obtained suggesting fluxonality between σ- and π-pyr in Zr complexes,[17] driving us to study the bonding of this ligand in the two coordination modes and to investigate the corresponding interconversion mechanism.

In this work we use ab initio[18] and DFT[19] calculations to study the bonding geometry of pyrrolyl ligands in monopyrrolyl, $[Zr(pyr')L_3]$, and bispyrrolyl, $[Zr(pyr')_2L_2]$, zirconium complexes and to investigate the mechanism for the interconversion between the σ and π coordination modes of the pyrrolyl ligand in those species. The complexes studied include chloride (L = Cl) and methyl ($L = CH_3$) as ancillary ligands and different pyrrolyl ligands, pyr′ (see Scheme 2).

Scheme 3

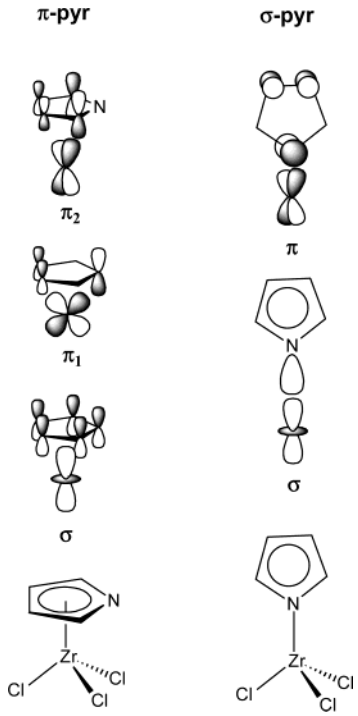

Results and Discussion

A comparative study of the bonding of a pyrrolyl ligand to a metal fragment in the two coordination modes (σ and π) was recently published for tungsten bispyrrolyl complexes, $[W(pyr')_2(CH_3)_2]$,[16] being qualitatively similar to what happens in a Zr complex. On one hand, for a π-pyr, the entire π system of this ligand is involved in the bonding, and, on the other, in a σ coordination the pyr−metal bond is based on the nitrogen lone pair. The relevant orbital interactions associated with each of those coordination modes for a $[Zr(pyr)Cl_3]$ model complex are depicted in Scheme 3 in a schematic and simplified way, based on extended Hückel (EH) calculations.[20,21]

In a π coordination, the pyr−Zr bond is based on three interactions, σ, π_1, and π_2 (left side of Scheme 3), resulting from the combination of the metal d orbitals and the pyr π orbitals with the right symmetry match. The overall bond can be view as the sum of three two-electron donations from the pyrrolyl to the metal, in a way that parallels what is well known for a η^5-Cp ligand.[22] For σ-pyr (right side of Scheme 3), the bond is essentially based on a strong σ interaction between the nitrogen lone pair and the metal d_{z^2} orbital, the pyr−Zr π donation, corresponding to interaction π in Scheme 3, being comparatively of small importance due to the poor overlap between the intervening fragment molecular orbitals. The overall (σ-pyr)−Zr bond results formally from two two-electron donations from the pyrrolyl to the metal. In a comparison between the two coordination modes, an electronically richer metallic fragment should exist in the π-pyr complex, but the overall pyr−Zr bond strength is roughly the same for the two coordination modes. This result is equivalent to what

(10) Tanski, J. M.; Parkin, G. *Organometallics* **2002**, *21*, 587.
(11) Jacony, D.; Floriani, C.; Chiesi-Villa, A.; Rizzoli, C. *J. Chem. Soc., Chem. Commun.* **1991**, 790.
(12) Hollis, T. K.; Wang, L.-S.; Tham, F. *J. Am. Chem. Soc.* **2000**, *122*, 11737.
(13) Bellemin-Laponnaz, S.; Lo, M. M.-C.; Peterson, T. H.; Allen, J. M.; Fu, G. C. *Organometallics* **2001**, *20*, 3453.
(14) Dias, A. R.; Galvão, A. M.; Galvão, A. C. *Collect. Czech. Chem. Commun.* **1998**, *63*, 182.
(15) Dias, A. R.; Galvão, A. M.; Galvão, A. C. *J. Organomet. Chem.* **2001**, *632*, 157.
(16) Ascenso, J. R.; Dias, A. R.; Ferreira, A. P.; Galvão, A. C.; Salema, M. S.; Veiros, L. F. *Inorg. Chim. Acta*, accepted.
(17) Ferreira, A. P. Ph.D. Thesis IST, Universidade Técnica de Lisboa, Lisbon, 2003 (in Portuguese).
(18) Hehre, W. J.; Radom, L.; Schleyer, P. v. R.; Pople, J. A. *Ab Initio Molecular Orbital Theory*; John Wiley & Sons: New York, 1986.
(19) Parr, R. G.; Yang, W. *Density Functional Theory of Atoms and Molecules*; Oxford University Press: New York, 1989.
(20) Hoffmann, R. *J. Chem. Phys.* **1963**, *39*, 1397.
(21) Hoffmann, R.; Lipscomb, W. N. *J. Chem. Phys.* **1962**, *36*, 2179.
(22) Albright, T. A.; Burdett, J. K.; Whangbo, M. H. *Orbital Interactions in Chemistry*; John Wiley & Sons: New York, 1985.

Scheme 4

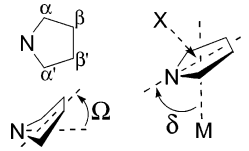

happens in tungsten pyrrolyl complexes[16] and indicates that similar pyr−metal bonds are obtained when the pyr coordination is based on one strong and one weak interaction (σ coordination) and when it is based on three interactions of intermediate strength (π coordination).

The degree of distortion on a pyr′ π coordination geometry is an important factor to evaluate the bonding of this ligand to the metal center, as normally some slippage is observed (see Introduction).[9] A number of geometrical parameters have been developed to characterize the distortion of a C_5 ring π coordinated to a metal,[23] and their use can be easily extended to a pyrrolyl ligand. Two such parameters are the folding angle, Ω (see Scheme 4), and the slip parameter, Δ. In a pyrrolyl NC_4 ring, Ω may be defined as the angle between the plane of the nitrogen and the two adjacent carbons (α) and the mean plane of the four carbon atoms. This angle measures the degree of folding of the ring, being 0° for a perfect η^5 coordination, while higher values denote a tendency toward η^3 coordination. In the case of a Cp ligand, for example, a typical folded η^3-Cp is normally associated with Ω values well over 10°.[24] The slip parameter, Δ, can be defined as the difference between the mean distance from the metal to the β ring carbons, and the mean distance from metal to the nitrogen and the two α carbons. Thus, a perfect η^5 coordination corresponds to $\Delta = 0$, and higher values indicate an increase of the $M-C_{\beta/\beta'}$ bond lengths and a shortening of the M−N distance, with the corresponding slipped η^3 coordination. A third and, perhaps, more intuitive parameter is the tilt angle, δ (see Scheme 4). It has been used to define the slippage degree of a NC_4 pyrrolyl ring[9] and is defined as the N−X−M angle, X being the ring centroid.[25] In fact, a continuous slippage (without folding) from a perfect η^5-pyr′ to a σ coordination of this ligand corresponds to a monotonic variation of δ from 90 to 0°.

Monopyrrolyl Complexes: [Zr(pyr′)L$_3$]. In a monopyrrolyl complex, [Zr(pyr′)L_3], two isomers may exist, depending on the pyrrolyl coordination mode, a π or a σ complex. The optimized geometries of the π and the σ isomers, as well as the corresponding transition states for the interconversion between the two, are presented in Figure 1 for the monopyrrolyl chloro complexes, [Zr(pyr′)Cl_3], with pyrrolyl (pyr = $NC_4H_4^-$) and 2,5-dimethylpyrrolyl (dmp = $NC_4Me_2H_2^-$). The pyr′ coordination parameters are also shown. Although there are no available X-ray structures to test the optimized geometries, the method and basis set used (see Computational Details) have proved well on the description

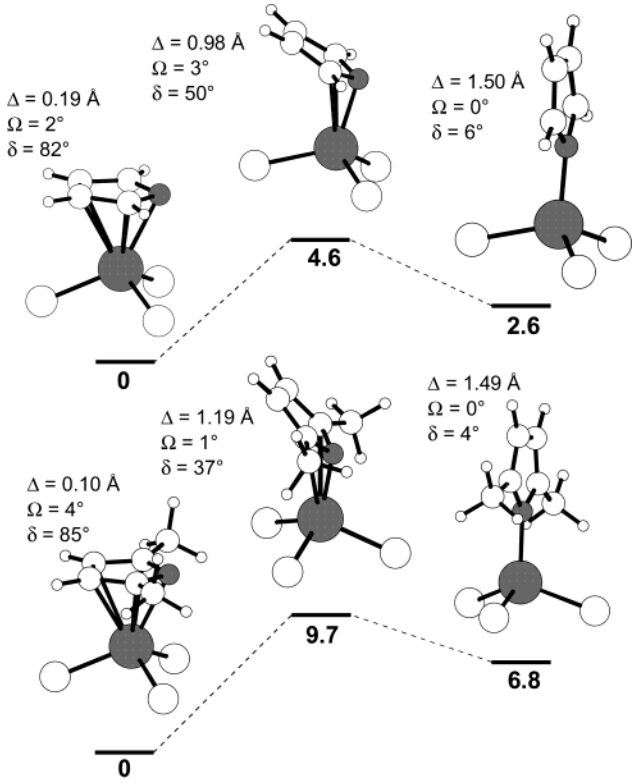

Figure 1. Optimized geometries (B3LYP) of the π and the σ complexes, [Zr(pyr′)Cl_3], and of the transition state for the interconversion between the two, for pyr (top) and dmp (bottom). The relative energies (bold, kcal mol^{-1}) and the pyr′ coordination parameters are presented. The Zr and N atoms are shaded.

of tungsten pyrrolyl complexes[16] and are equivalent to what has been used by Parkin et al. for Zr complexes.[10] In this elegant work, π and σ [Zr{NC_4(aryl)$_2H_2$}(NMe_3)$_3$] complexes (aryl = Ph, Xyl) were synthesized and structurally characterized by X-ray diffraction.

The geometries calculated for the pyrrolyl species are very similar to the ones obtained for the dmp complexes with a maximum deviation of 0.06 Å and 4° for the bond distances and angles around the metal coordination sphere. The π complexes present a typical piano stool geometry with X−Zr−Cl angles between 110° and 115° (X being the NC_4 ring centroid) and Zr−Cl distances of 2.37 Å. The pyr′ ligands coordinate in a π fashion, with the five ring atoms involved in the bond to the metal, as shown by Zr−N/C distances $d_{Zr-N} = 2.37$, 2.42 Å and $d_{Zr-C} = 2.47-2.64$ Å, well within the bonding values. The result is a slightly slipped η^5 coordination of the pyr′ ligand with tilt angles (δ) of 82° and 85° for the pyr and the dmp complexes, respectively, and slip parameters (Δ) of 0.19 and 0.10 Å, by the same order. However, a rather flat ring is observed for all the species presented in Figure 1, the maximum folding angle (Ω) obtained being 4° for [Zr(π-dmp)Cl_3]. This indicates that the interconversion process between the π and the σ isomers of these complexes occurs via ring slippage without significant ring folding. Interestingly, the coordination geometry calculated for the π complexes of Figure 1 compares remarkably well with the X-ray structure of [Zr(π-$NC_4Ph_2H_2$)(NMe_3)$_3$][10] ($\delta = 84°$, $\Omega = 4°$, $\Delta = 0.13$ Å, $d_{Zr-N} = 2.48$ Å, $d_{Zr-C} = 2.56-2.67$ Å), especially taking into account the differences between the species.

(23) Faller, J. W.; Crabtree, R. H.; Habib A. *Organometallics* **1985**, *4*, 929.

(24) Veiros, L. F. *Organometallics* **2000**, *19*, 5549.

(25) In the case of a slippage approaching the N and the metal in a symmetrical way ($d_{M-C\alpha} = d_{M-C\alpha'}$, $d_{M-C\beta} = d_{M-C\beta'}$): $\delta = 90° - \psi$, where ψ is the angle slip, defined for C_5 rings: Honan, M. B.; Atwood, J. L.; Bernal, I. Herrmann, W. A. *J. Organomet. Chem.* **1979**, *179*, 403.

The σ complexes of Figure 1 present slightly distorted tetrahedral geometries with N−Zr−Cl angles between 108° and 113° and distances around the metal coordination sphere well within the bonding range (d_{Zr-N} = 2.04, 2.05 Å, d_{Zr-Cl} = 2.34−2.35 Å). The pyrrolyl ligands coordinate in a clearly σ mode, as stated by the large values of the slip parameter, Δ close to 1.5 Å, and by tilt angles approaching zero, δ = 6° and 4° for the pyr and the dmp complexes, respectively. The geometry of the σ-pyr′ coordination compares well with the X-ray structure obtained for [Zr(σ-$NC_4Xyl_2H_2$)$(NMe_3)_3$][10] (δ = 16°, Ω = 2°, Δ = 1.44 Å, d_{Zr-N} = 2.22 Å, N−Zr−N = 105−117°) given the differences between the complexes, especially the bulkiness of the pyrrolyl α substituents: hydrogen or methyl in this work and 2,4-xylyl in the X-ray structure.

One interesting aspect arising from the comparison between the pyrrolyl coordination geometry in the π and the σ isomers is the shortening of the Zr−N distance from 2.37 to 2.42 Å in a π-pyr′ to 2.04−2.05 Å in a σ bonding. This is a direct consequence of the σ interaction between the nitrogen lone pair and the metal d_{z^2} orbital, obtained in a σ coordination, as previously discussed while addressing the qualitative nature of the pyr−M bond (see Scheme 3). The electronic basis of this effect is confirmed by the calculated Wiberg indices (WI)[26] for the Zr−N bonds in the various species. These bond strength indicators rise from 0.26 to 0.28 in the π-pyr′ complexes to 0.71 in the σ isomers, showing that the shortening of the Zr−N bond length corresponds to an intrinsic strengthening of the bond. There is also a slight shortening of the Zr−Cl bonds, going from the π (2.36−2.37 Å) to the σ complexes (2.34−2.35 Å). However, comparable Wiberg indices are obtained for those bonds in the two types of complexes (1.03−1.05 for the π species and 1.03 for the σ isomers), suggesting that this geometrical change is of stereochemical, rather than electronic, nature, resulting, probably, from a less crowded metal coordination sphere in the σ complexes.

The transition states calculated for the slippage from a π to a σ coordination of the pyr′ ligands present geometrical and electronic parameters that are intermediate between the ones obtained for the two types of species. The geometry of the pyr′ ligands is flat, but considerably slipped, as shown by the corresponding parameters, δ = 50° and 37°, Ω = 3° and 1°, Δ = 0.98 and 1.19 Å, for pyr and dmp, respectively. The distance from the metal to the β carbons of the pyrrolyl ring is clearly outside the bonding range (3.5−3.9 Å), indicating that the M−$C_{\beta/\beta'}$ bond breaking is already completed in the transition state. The Zr−N bond is shorter (2.10 Å for pyr and 2.08 Å for dmp) and stronger (WI = 0.53 and 0.58 for pyr and dmp, respectively) than the ones existing in the π-pyr′ complexes (see above), and the M−$C_{\alpha/\alpha'}$ interaction can be classified as a weak bond, significantly longer (2.68−3.08 Å) and weaker (WI = 0.07−0.17) than the ones existing in the π species ($d_{Zr-C\alpha/\alpha'}$ = 2.47−2.50 Å, and $WI_{Zr-C\alpha/\alpha'}$ = 0.20−0.21).

The slippage from a π-pyr′ to a σ-pyr′ is an endothermic process for the species depicted in Figure 1, as the σ complexes are less stable than the π species. The calculated energy difference between the two isomers is significantly higher for the α-substituted pyrrolyl, dmp (ΔE = 6.8 kcal mol^{-1}), than for pyr (ΔE = 2.6 kcal mol^{-1}), corroborating the fact, empirically well known, that substituents on the pyrrolyl α carbons tend to favor a π coordination mode of the ligand.[9,10] This is reflected in the two energy profiles of Figure 1, with a higher activation energy for the slippage of the dmp ligand (E_a = 9.7 kcal mol^{-1}) when compared with the corresponding value for the pyr complexes (E_a = 4.6 kcal mol^{-1}). The nature of the transition state is another consequence of this result, being much closer to the σ isomer in the case of dmp than in that of pyr, both in energetic terms, as stated by the energy differences between the transition state and the minima for the two ligands (Figure 1), as well as geometrically, since the transition state for dmp has a shorter Zr−N distance, a narrower tilt angle (δ), and a higher slip parameter (Δ) than the transition state for pyr. An electronic reason can be found for the stability difference obtained for the two types of complexes, as an electronically poorer metal center results in a σ-pyr′ species. This was anticipated by the EH calculations and is confirmed by the metal charges (C_{Zr}) calculated by means of a natural population analysis (NPA),[27] increasing from 1.33/1.34 in the π-pyr′ complexes to 1.53/1.56 in the σ-pyr′ species.

The small values obtained for the activation energy associated with the slippage process suggest that fluxionality between the two isomers may occur in solution, even at room temperature, especially for the pyr complex.

Qualitatively similar results are obtained for the analogous methyl π and σ complexes, [Zr(pyr′)$(CH_3)_3$]. However, the energy differences between the two isomers with those ancillary ligands are much lower, being practically isoenergetic (within 0.6 kcal mol^{-1}) for pyr, while for dmp the π complex is only 2.6 kcal mol^{-1} more stable than its σ isomer. This suggests that with L = CH_3 the metal is less affected by the electronic density depletion associated with the slippage from π-pyr′ to σ-pyr′.

Bispyrrolyl Complexes: [Zr(pyr′)$_2$L$_2$]. In the case of the bispyrrolyl complexes, [Zr(pyr′)$_2$L$_2$], three different isomers may occur, depending on the coordination mode of each pyrrolyl ligand. A π/π complex results when both ligands coordinate in a π fashion, a π/σ species exists with one π-pyr′ and one σ-pyr′, and, finally, a σ/σ isomer arises when both pyrrolyl ligands are bonded in a σ mode. The optimized geometries for the three isomers of the dichloro complexes, [Zr(pyr′)$_2$Cl$_2$], for pyr′ = pyr and dmp, are depicted in Figure 2. The transition states corresponding to the successive slippage of each pyr′ ligand from a π to a σ coordination are also shown, as well as the relative energies and the pyr′ coordination parameters.

Qualitatively similar geometries are obtained for the complexes with pyr and dmp, with a maximum difference of 0.07 Å and 5° for the relevant bond distances and angles around the metal coordination sphere. The

(26) Wiberg, K. B. *Tetrahedron* **1968**, *24*, 1083.

(27) (a) Carpenter, J. E.; Weinhold, F. *J. Mol. Struct. (THEOCHEM)* **1988**, *169*, 41. (b) Carpenter, J. E. Ph.D. Thesis, University of Wisconsin (Madison WI), 1987. (c) Foster, J. P.; Weinhold, F. *J. Am. Chem. Soc.* **1980**, *102*, 7211. (d) Reed, A. E.; Weinhold, F. *J. Chem. Phys.* **1983**, *78*, 4066. (e) Reed, A. E.; Weinhold, F. *J. Chem. Phys.* **1983**, *78*, 1736. (f) Reed, A. E.; Weinstock, R. B.; Weinhold, F. *J. Chem. Phys.* **1985**, *83*, 735. (g) Reed, A. E.; Curtiss, L. A.; Weinhold, F. *Chem. Rev.* **1988**, *88*, 899. (h) Weinhold, F.; Carpenter, J. E. *The Structure of Small Molecules and Ions*; Plenum: New York, 1988; p 227.

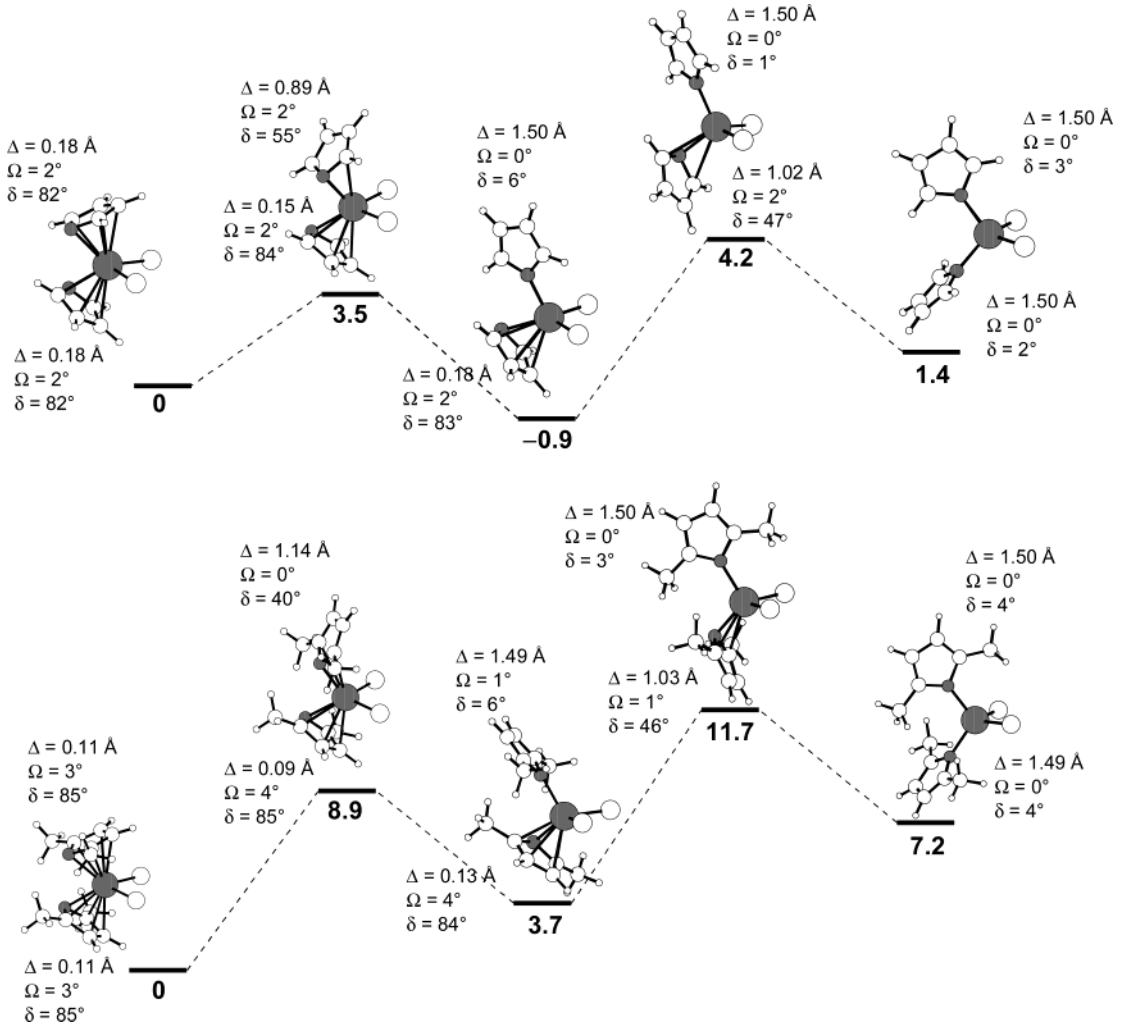

Figure 2. Optimized geometries (B3LYP) of the π/π, the π/σ, and the σ/σ complexes, $[Zr(pyr')_2Cl_2]$, and of the transition states for the corresponding interconversions, for pyr (top) and dmp (bottom). The relative energies (bold, kcal mol^{-1}) and the pyr′ coordination parameters are presented. The Zr and N atoms are shaded.

π/π complexes present a pseudo-tetrahedral geometry, with two π-pyr′ and two Cl ligands occupying the four coordination positions, and bond angles (X−Zr−X = 132°, Cl−Zr−Cl = 98°) and distances (Zr−C = 2.48−2.66 Å, Zr−N = 2.41, 2.45 Å, Zr−Cl = 2.42−2.43 Å) within the typical values for a Zr^{IV} bent metallocene.[8] A slightly slipped η^5 coordination of the pyr′ ligands is observed, as shown by the corresponding parameters (δ, Δ, and Ω), but the NC_4 ring remains essentially unfolded during the entire slippage process, for both the pyr and the dmp complexes. The larger folding angle considering all the structures of Figure 2 is only 4°. The general features of the geometries optimized for the π/π complexes compare well with the X-ray structure of [Zr(π-$NC_4Ph_2H_2$)Cl_2],[10] especially taking into account the difference between the pyr′ substituents. The experimental values for the angles around the metal (X−Zr−X = 128°, Cl−Zr−Cl = 98°) and the Zr−Cl bond lengths (2.41 Å) are similar to the calculated ones for the pyr and dmp species.

In the optimized π/σ complexes, one pyr′ ligand binds in a π fashion, while the other coordinates by means of the nitrogen lone pair, in a σ mode. The overall geometry around the metal may be envisaged as a piano stool, with the three legs being the two Cl and the σ-pyr′ ligand. These species are, thus, equivalent, in geometrical terms, to the [Zr(π-pyr′)Cl_3] complexes discussed before, considering that one Cl ligand is replaced by a σ-pyr′. This is shown, for example, by the angles X−Zr−L, X being the NC_4 ring centroid and L being Cl or the σ-pyr′ nitrogen, falling in a range (110−116°) similar to what happened for X−Zr−Cl in the monopyrrolyl π complexes. A slightly slipped η^5 coordination is observed for the π-pyr′ ligand, as shown by large tilt angles, close to 90°, and small slip parameters (Δ < 0.2 Å). The second pyr′ adopts a clear σ coordination with very narrow tilt angles, δ = 6°, and slip parameters close to Δ = 1.5 Å. The Zr−N bond for the σ-pyr′ (d = 2.07 and 2.10 Å and WI = 0.67 and 0.62, for pyr and dmp, respectively) is much shorter and stronger than the ones existing in the π-pyr′ ligands (d_{Zr-N} = 2.41 − 2.45 Å and WI = 0.25−0.28). The Zr−Cl bond distances in the π/σ species (2.38 Å) are shorter than the ones obtained for the π/π isomers (2.42−2.43 Å), but the corresponding Wiberg indices do not show any clear tendency, suggesting that stereochemical causes may be responsible for the observed differences. In fact, a very narrow range of Zr−Cl Wiberg indices is found for all the species in Figure 2, WI_{Zr-Cl} = 0.95−1.04.

The σ/σ species present a slightly distorted tetrahedral geometry around the metal, with N−Zr−N angles of 106° and 108° and Cl−Zr−Cl of 112° and 107° for

pyr and dmp, respectively, being thus very close to the value of a perfect tetrahedron (109.5°). Both pyr′ ligands are coordinated in a unambiguous σ mode, and the corresponding parameters have values equivalent to all the σ-pyr′ discussed so far ($\delta \leq 4°$ and $\Delta \approx 1.5$ Å). The trends observed going from the π/π to the π/σ complexes are repeated with the slippage of the second pyr′ ligand from a π to a σ coordination.

The transition states for the slippage of the pyr′ ligand have geometries that are intermediate between the two corresponding isomers. Thus, a flat ($\Omega \leq 2°$) η^3 coordination of the slipping ligand is found, with the characteristic tilt angles ($\delta = 40-55°$) and slip parameters ($\Delta = 0.9-1.1$ Å). The distances from the metal to the two β carbon atoms of the slipping pyr′ are beyond bonding values ($d_{Zr-C\beta/\beta'} > 3.3$ Å), showing that the bond breaking associated with slippage from a π to a σ coordination is completed in the transition state. The Zr−N bonds in the transition states are shorter ($d = 2.11-2.16$ Å) and stronger (WI = 0.46−0.54) than the ones present in a π-pyr′, but are still far from the values characteristic of a σ coordination. The two $Zr-C_{\alpha/\alpha'}$ bonds present in a π coordination are considerably weakened for the slipping ligand in the transition state, with long bond lengths ($d = 2.56-2.95$ Å) and low Wiberg indices (WI = 0.09−0.20) characteristic of weak interactions, but still justifying the designation η^3 for the pyr′ coordination mode.

The three isomers of the pyrrolyl complexes (pyr′ = pyr) in Figure 2 have comparable stabilities. The maximum energy difference is 2.3 kcal mol^{-1}, showing the absence of a marked preference for any of the species. In this case, the depletion of the electronic density on the metal with the number of σ-coordinated pyr ligands shown by the metal NPA charges, $C_{Zr} = 1.37$ (π/π), 1.59 (π/σ), and 1.80 (σ/σ), is balanced by the release of the interligand repulsion around the metal, differing from what happened in the monopyrrolyl complexes, [Zr(pyr)Cl$_3$], where the first factor prevailed. This reflects the differences between the steric demands of a Cl and a σ-pyr ligand. The values obtained for the activation energies associated with the slippage process are small ($E_a \leq 5.1$ kcal mol^{-1}), suggesting that fluxionality between the three isomers should occur in solution, even at room temperature.

Although small, the energetic differences obtained for the three isomers of the dmp complex show a clear trend of an increasing stability with the number of π-coordinated dmp ligands. This results from the known effect of substituents in the pyrrolyl α carbons, disfavoring the σ coordination of those ligands,[9,10] already discussed for the monopyrrolyl complexes. This is also shown by the activation energies for the slippage process with considerably higher values for the slippage from the π/π species to the π/σ complex, and from this to the σ/σ species, for dmp (8.9 and 8.0 kcal mol^{-1}), when compared with pyr (3.5 and 5.1 kcal mol^{-1}). In fact, the transition states are closer to the corresponding σ-pyr′ product in the case of the dmp complexes than in the case of pyr, both in energy (see Figure 2 values) and geometrically. Taking the tilt angle of the slipping pyr′ ligand, for example, systematically lower values, and, thus, closer to a σ coordination, are found for dmp, especially for the slippage of the first pyr′ ligand, where the steric constraints are more demanding: $\delta = 55°$ and 40° for pyr and dmp, respectively. The activation energies calculated for [Zr(dmp)$_2$Cl$_2$] are still reachable, and thus, fluxionality may occur in solution, if not between the three isomers, at least involving the more stable ones, that is, the π/π and the π/σ complexes.

Interestingly, for the methyl complexes, [Zr(pyr′)$_2$(CH$_3$)$_2$], qualitatively equivalent results are obtained. The values calculated for the relative stability of the isomers are within 2 kcal mol^{-1} of the ones presented by the chloro complexes of Figure 2.

The existence of ^{13}C NMR data for the bispyrrolyl complexes, [Zr(pyr′)$_2$Cl$_2$],[17] prompted us to further investigate the possibility of a fluxional behavior of these species in solution, involving the slippage of the pyr′ ligand between the π and the σ coordination modes, and the corresponding interconversion between the different isomers. This was done through the calculation of the C chemical shifts by means of the gauge independent atomic orbitals (GIAO)[28] method (see Computational Details). In fact, available ^{13}C NMR data, and not only ^{1}H NMR, are crucial for such a study, since only in the first case are the differences between the chemical shifts of unequivalent atoms sufficiently high to support the conclusions that may be drawn from the comparison of experimental and calculated data. The importance of this study is further enhanced by the fact that, in the absence of X-ray structures, the coordination mode of the pyrrolyl ligands is often determined by means of NMR data.[9,14-16,29] It is, thus, essential to know if the spectrum recorded in solution corresponds to one well-defined molecule, or if it corresponds to a mean spectrum associated with a fluxional process involving two or more isomers. Special care must be taken with the values for the ^{13}C chemical shifts for the α and the β carbon atoms of pyrrolyl, traditionally assumed to correspond to a π or a σ coordination. Even in the case of complexes with determined X-ray structures, the assignment of the chemical shifts obtained from spectra recorded in solution to the coordination mode shown by the pyr′ ligand in the crystal structure is not unequivocal. Several species may coexist in solution, while the one that crystallizes is dictated by factors such as solubility differences and crystal-packing effects. The recent results obtained by Parkin et al.[10] with [Zr{NC$_4$(aryl)$_2$H$_2$}(NMe$_2$)$_3$] (aryl = Ph, Xyl) strongly support this conclusion. The X-ray structures of those complexes correspond to a π complex for aryl = Ph and to the σ isomer when aryl = Xyl. However, the ^{13}C chemical shifts recorded in solution are practically equal in the two complexes, for both the α (144 and 140 ppm for aryl = Ph and Xyl, respectively) and the β carbon atoms (111 and 113 ppm for aryl = Ph and Xyl, respectively), suggesting that the same fluxional process may be occurring in solution for both cases.

The accuracy of the calculated chemical shifts has to be tested with a species without fluxionally between a π and a σ coordination of the π ligand, but, at the same

(28) (a) Wolinski, K.; Hilton, J. F.; Pulay, P. *J. Am. Chem. Soc.* **1990**, *112*, 8251. (b) Dodds, J. L.; McWeeny, R.; Sadlej, A. J. *Mol. Phys.* **1980**, *41*, 1419. (c) Ditchfield, R. *Mol. Phys.* **1974**, *27*, 789. (d) McWeeny, R. *Phys. Rev.* **1962**, *126*, 1028. (e) London, F. *J. Phys. Radium, Paris* **1937**, *8*, 397.

(29) Kuhn, N.; Stubenrauch, S.; Boese, R.; Blaser, D. *J. Organomet. Chem.* **1992**, *440*, 289.

time, it should be as similar as possible to the pyr′ complexes studied here. We chose the analogous biscyclopentadienyl complex, $[ZrCp_2(CH_3)_2]$. This complex has a determined X-ray structure[30] and published ^{13}C NMR data.[31] A geometry optimization was performed for this complex at the same level of theory as the one used for the pyr′ complexes. The calculated geometry is very similar to the experimental one, with mean and maximum absolute deviations of 0.04 and 0.06 Å for the Zr−C distances. The L−Zr−L angles, characteristic of the bent metallocene pseudo-tetrahedral structure, are also well described with 133° (calc) and 132° (expt) for Cp−Zr−Cp and 99° (calc) and 96° (expt) for CH_3−Zr−CH_3. The GIAO calculated chemical shift for the cyclopentadienyl, 114 ppm, compares rather well with the experimental value of 110 ppm, representing an overestimation of 4%. Calculated ^{13}C chemical shifts at this level of theory have been used previously to evaluate a possible fluxional process in tungsten bispyrrolyl complexes.[16]

Considering, for example, the ^{13}C NMR chemical shifts of the dmp α carbon atoms of complex $[Zr(dmp)_2Cl_2]$, the experimental value is 147 ppm,[17] while the calculated ones are 153 ppm for the π/π complex and 145 ppm for the σ/σ species. Taking into account that a small overestimation is to be expected in the calculated shifts (see the results on the Cp complex, above), the calculated value for the π/π isomer reproduces rather well the experimental one. In fact, correcting the calculated value for a 4% overestimation, the experimental value is reproduced exactly. This suggests that the π/π isomer should be the predominant species in solution and gives no indication of any fluxional behavior for $[Zr(dmp)_2Cl_2]$ in solution. For the analogous pyr complex, $[Zr(pyr)_2Cl_2]$, the experimental ^{13}C chemical shift for the pyr α carbons is 135 ppm. The corresponding calculated values are 144 ppm for the π/π isomer and 132 ppm for the σ/σ species, and the mean value for the π/σ complex is 139 ppm. In this case, the calculated chemical shifts seem to indicate the existence of a fluxionality process in solution, involving the three isomers. This is in good accordance with the activation energies calculated for the slippage processes in the pyr and dmp complexes (Figure 2), where considerably lower values were obtained for the pyr complex ($E_a \leq 5.1$ kcal mol^{-1}) than for the dmp species ($E_a \geq 8.0$ kcal mol^{-1}).

$[Zr(NC_4Me_2EtH)_2Me_2]$: A Case Study. Given the asymmetric nature of 2,4-dimethyl-3-ethylpyrrolyl (dmep, see Scheme 2), the bis(π-pyr′) dimethyl complex, $[Zr(\pi\text{-dmep})_2(CH_3)_2]$, presents two stereoisomers, a chiral form, *rac*, and a *meso* form, both schematically draw in Scheme 5. Preliminary ^1H NMR results[17] point toward the existence of fluxionality between the *rac* and the *meso* forms in solution at room temperature and prompt us to theoretically study the corresponding mechanism and find in which way, if any, it relates with the slippage of the dmep ligands from a π to a σ coordination. A similar isomerization process have been recently observed with related Zr and Hf complexes, $[M(\pi\text{-}PC_4PhMe_2H)_2Cl_2]$.[12,13] In this case, the π ligand is a substituted phospholyl, PC_4PhMe_2H, and, thus, closely related to dmep, since both are asymmetric heterocyclic ligands.

Scheme 5

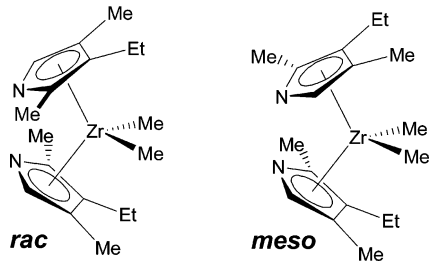

A first stage for the investigation of all the isomers of $[Zr(dmep)_2(CH_3)_2]$ and their interconversion mechanisms consisted in the study of the successive slippage of each of the dmep ligands in the *rac* and the *meso* forms of the π/π species, similarly to what has been done with the mono- and bispyrrolyl chloro complexes, discussed above. The corresponding energy profiles, as well as the optimized structures of the intervening species are presented in Figure 3 with the coordination parameters of the dmep ligands.

A complete equivalence is observed between the optimized structures for the π/π, the π/σ, and the σ/σ dmep complexes and the ones previously obtained for the bis(pyr′) chloro complexes, $[Zr(pyr')_2Cl_2]$. The π/π species have the pseudo-tetrahedral geometries typical of bent metallocenes with the four coordination positions occupied by two π-dmep and two methyl ligands; the π/σ complexes present asymmetric piano stool geometries with one π-dmep, the three legs being formed by the two methyls and the σ-dmep ligand; finally, the σ/σ isomers have almost perfect tetrahedral geometries with two σ-dmep and two methyl ligands. The π-dmep ligands coordinate in a slightly distorted η^5 mode, with coordination parameters ($\Delta = 0.22-0.25$ Å, $\delta = 80-81°$) close to the ones calculated for the pyr and dmp species. The σ coordination mode for dmep complexes of Figure 3 is also characterized by parameters ($\Delta = 1.50-1.52$ Å, $\delta = 2-8°$) similar to the ones obtained for the chloro complexes. The same happens with the transition states with a η^3 coordination of the slipping dmep ligand, intermediate between the π and the σ bonding modes ($\Delta = 0.93-1.20$ Å, $\delta = 38-52°$). The dmep ligands remain practically flat during the slippage process in all cases, $\Omega \leq 2°$, and the electronic richness of the metal decreases with the number of σ-dmep ligands, as shown by the Zr NPA charges: 1.82/1.83 for the π/π species, 2.02/2.04 for the π/σ complexes, and 2.14/2.16 for the σ/σ isomers. The Zr−N bonds for the π-coordinated dmep ligands are longer ($d = 2.34-2.41$ Å) and weaker (WI = 0.26−0.29) than the ones presented when those ligands are σ bonded to the metal ($d = 2.09-2.12$ Å, WI = 0.58−0.61). The Zr−CH_3 bonds become shorter with the number of σ-bonded dmep ligands, falling from 2.27 Å in the π/π species to 2.24 Å in the π/σ complexes, and to 2.23 Å in the σ/σ isomers. Contrary to what was found for the chloro complexes, in the case of $[Zr(dmep)_2(CH_3)_2]$ the Zr−CH_3 Wiberg indices show a clear trend, increasing along the series (WI = 0.68−0.69, 0.71−0.73, and 0.74−0.76 for the π/π, the π/σ, and the σ/σ complexes, respectively) and indi-

(30) Hunter, W. E.; Hrncir, D. C.; Bynum, R. V.; Penttila, R. A.; Atwood, J. L. *Organometallics* **1983**, *2*, 750.

(31) Jezequel, M.; Dufaud, V.; Ruiz-Garcia, M. J.; Carrillo-Hermosilla, F.; Neugebauer, U.: Niccolai, G. P.; Lefebvre, F.; Bayard, F.; Corker, J.; Fiddy, S.; Evans, J.; Broyer, J.-P.; Malinge, J.; Basset, J.-M. *J. Am. Chem. Soc.* **2001**, *123*, 3520.

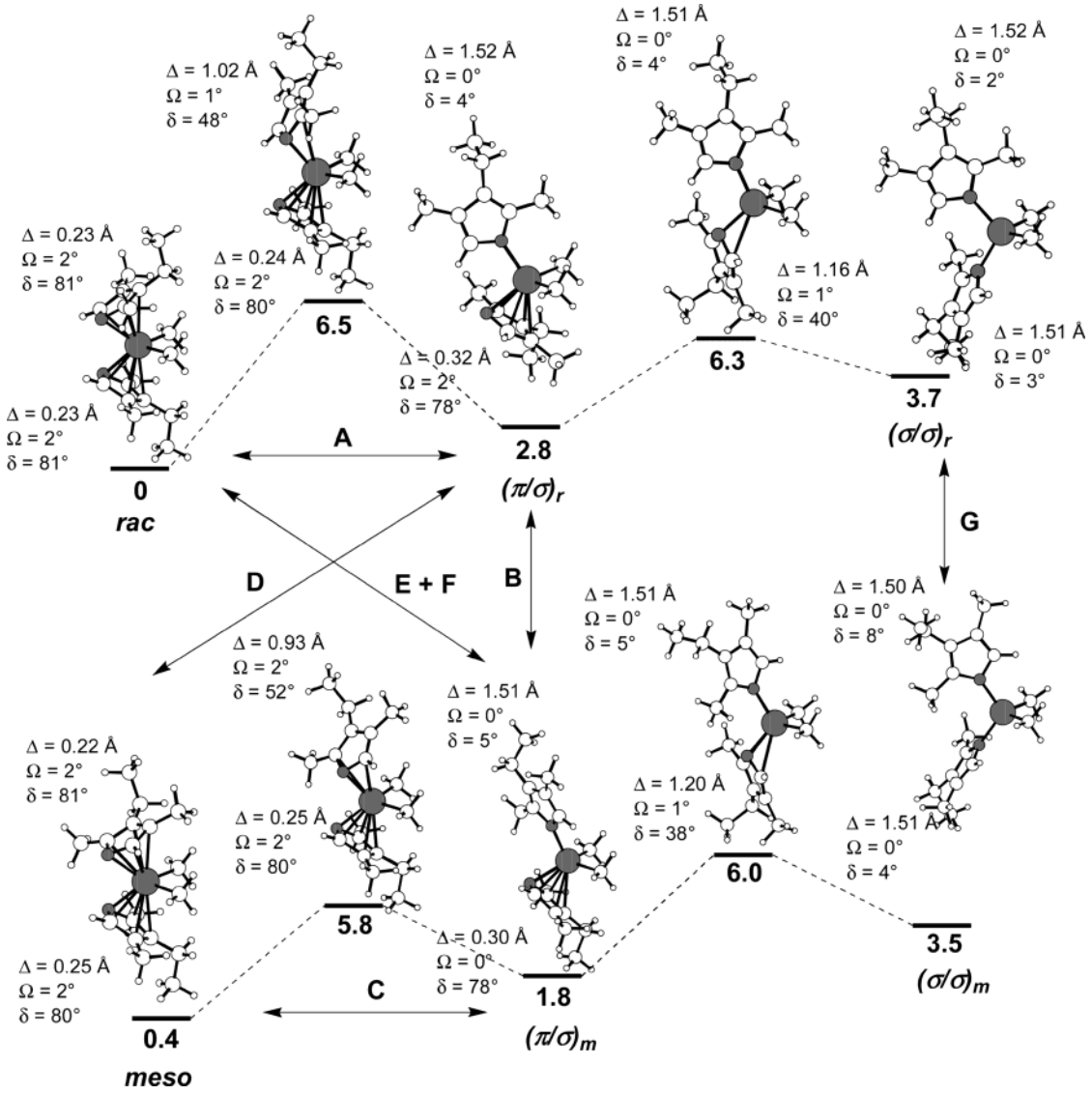

Figure 3. Calculated mechanism (B3LYP) for the successive slippage of each dmep ligand for the *rac* (top) and the *meso* (bottom) forms of $[Zr(\pi\text{-dmep})_2(CH_3)_2]$. The optimized geometries of the π/π, the π/σ, and the σ/σ complexes and of the transition states for the corresponding interconversions are presented, as well as the relative energies (bold, kcal mol^{-1}) and the dmep coordination parameters. The Zr and N atoms are shaded.

cating an electronic factor determining the strengthening of those bonds. In fact, with methyl rather than chloride as an ancillary ligand (L), the Zr−L bond compensates more efficiently the electronic density loss at the metal center with an increasing number of σ-coordinated ligands. The Zr charge increases 27% going from the π/π to the σ/σ isomers of $[Zr(dmp)_2Cl_2]$, while the corresponding increase in the methyl complexes of Figure 3 is only 18%. A similar trend is observed with the pyr and dmp methyl complexes.

The stability of the different isomers in Figure 3 decreases with the number of σ-coordinated dmep ligands. The π/σ species are 1.4 and 2.8 kcal mol^{-1} less stable than the corresponding π/π complex, for $(\pi/\sigma)_m$ and $(\pi/\sigma)_r$, respectively, and the equivalent energy differences for the σ/σ isomers are 3.1 kcal mol^{-1} for $(\sigma/\sigma)_m$ and 3.7 kcal mol^{-1} for $(\sigma/\sigma)_r$. A similar trend was found for the $[Zr(dmp)_2Cl_2]$ complexes, but, in this case, the destabilization associated with the slippage of dmp from a π to a σ coordination is considerably higher. Two reasons may be pointed out to explain this result. On one hand, there is a more effective compensation of the metal electronic loss associated with the slippage when the ancillary ligands are methyl (see above), and, on the other, the σ coordination of the dmep is less disfavored than that of dmp, since the dmep has one α substituent, i.e., one methyl group in one α carbon of the pyrrolyl ring, while dmp has two. This difference is reflected in the stability of the transition states associated with the slippage process and, thus, in the corresponding activation energies. These are 5.4 and 6.5 kcal mol^{-1} for the slippage of the first dmep ligand and 3.5 and 4.2 kcal mol^{-1} for the slippage of the second dmep ligand, while in the case of the dmp dichloro complex the corresponding values were 8.9 and 8.0 kcal mol^{-1}. The slippage process is, thus, considerably easier for $[Zr(dmep)_2(CH_3)_2]$, and the values calculated for the activation energy suggest the possibility of fluxionality in solution, even at room temperature.

Another interesting result is the relative stability of the two π/π stereoisomers, the *rac* and the *meso* forms. The *rac* isomer is slightly more stable (0.4 kcal mol^{-1}),

Scheme 6

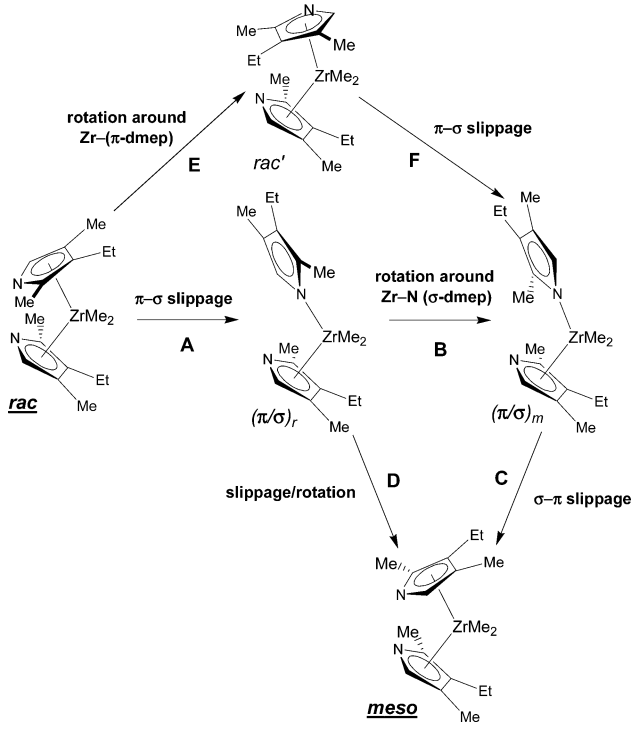

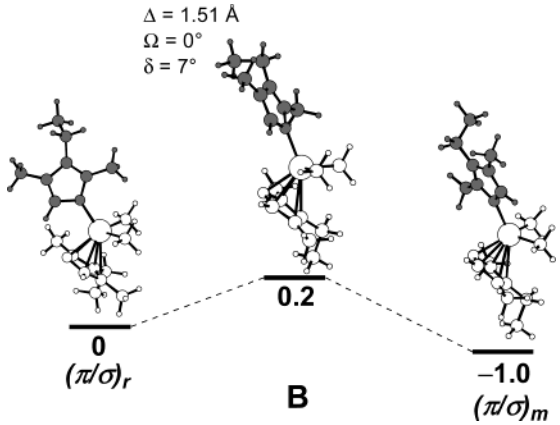

Figure 4. Energy profile (B3LYP) for the rotation of the σ-dmep ligand from $(\pi/\sigma)_r$ to $(\pi/\sigma)_m$ (step B). The relative energies (bold, kcal mol^{-1}) and the coordination parameters of the rotating dmep ligand (shaded) in the transition state are presented.

and from the difference calculated for the corresponding free energy a *rac*/*meso* ratio of 4:1 is obtained. This same ratio was obtained for the related phospholyl complex $[Zr(\pi\text{-}PC_4PhMe_2H)_2Cl_2]$, after washing the crude product with pentane.[12] The *rac*/*meso* ratio for this Zr phospholyl complex was found to stabilize at lower values for other solvents, 1.7:1 in $CDCl_3$[12] and 1.9:1 in benzene.[13]

A *rac*/*meso* isomerization process, for the dmep complex studied here, means that the two energy profiles of Figure 3 are connected in one or more ways. In other words, there must be interconversion between the minima in the two energy profiles. Given the difficulty of visualization of such a process, due to the complexity of the species involved and to the mechanism itself, some considerations are necessary. In all the relevant illustrations, Figures 3−7 and Scheme 6, the molecules are orientated in a way that the slipping or rotating dmep ligand is always the top one, except for the second slipping dmep in the interconversion between the π/σ and the σ/σ species in Figure 3. The designation of the elemental steps important to the mechanism (A to G) is maintained in the three illustrations.

Three general paths may be envisaged for the interconversion between the *rac* and the *meso* forms of $[Zr(\pi\text{-dmep})_2(CH_3)_2]$ through the π/σ species, as shown in Scheme 6. Starting, for example, from the *rac* form, one possibility is the $\pi-\sigma$ slippage of one dmep ligand, reaching $(\pi/\sigma)_r$, corresponding to the first slippage on the top of Figure 3 (step A). Then, a rotation around the Zr−N bond of the σ-dmep ligand (step B) will yield $(\pi/\sigma)_m$, and, finally, the slippage of the σ-dmep back to a π coordination (step C) yields the *meso* form. This is, thus, a mechanism involving three steps, A+B+C, corresponding to the successive slippage, rotation, and slippage again of the dmep ligand. The initial slippage step (A) has been previously discussed while analyzing the interconversion between the π and the σ coordination modes of the dmep ligand. The second step (B) corresponds to a rotation around a Zr−N σ bond and connects the π/σ isomers of the two energy profiles of Figure 3. The σ-dmep ligand rotates from a conformation where the α methyl group lies on the same side of the two methyl ligands, in $(\pi/\sigma)_r$, to another where the α methyl group is on the opposite side with respect to the two ancillary CH_3 ligands, in $(\pi/\sigma)_m$. Step B is depicted in Figure 4, with the optimized structures of the intervening species and the coordination parameters of the rotating dmep in the transition state. These parameters show a σ-bonded dmep, with a coordination geometry completely equivalent to all the σ-pyr′ ligands reported here. The third and last step of the mechanism is the slippage of the σ-dmep from a σ coordination in $(\pi/\sigma)_m$ to a π coordination in the *meso* form of $[Zr(\pi\text{-dmep})_2(CH_3)_2]$. This is the first slippage step on the bottom energy profile of Figure 3 and has been previously discussed. The rate-limiting step for this mechanism is step A, with a 6.5 kcal mol^{-1} activation energy. The second step (B) is comparatively facile (E_a = 0.2 kcal mol^{-1}) since it corresponds to a rotation around a σ bond. The last step has an intermediate activation energy, 4.0 kcal mol^{-1}, since although it corresponds to a slippage between the two coordination modes of dmep, such as A, it is reversed and, thus, starts from the less stable isomer, the π/σ species.

Another possible mechanism for the *rac*/*meso* isomerization considered in Scheme 6 has two steps. The first is common between this and the previous mechanism and corresponds to the slippage of one dmep, transforming the *rac* form of $[Zr(\pi\text{-dmep})_2(CH_3)_2]$ into $(\pi/\sigma)_r$; this is step A. A second step (D) is the fusion of steps B and C of the previous mechanism and corresponds to a simultaneous slippage and rotation of the σ-dmep ligand in $(\pi/\sigma)_r$, leading directly to the final *meso* product. The energy profile of this step is represented in Figure 5, with the optimized geometries of the intervening species and the coordination parameters of the slipping dmep in the transition state. Step D is a "diagonal" link between the two energy profiles of Figure 3, and the coordination geometry of the slipping and rotating dmep in the transition state is completely equivalent to what was found in all the slippage transition states, as shown

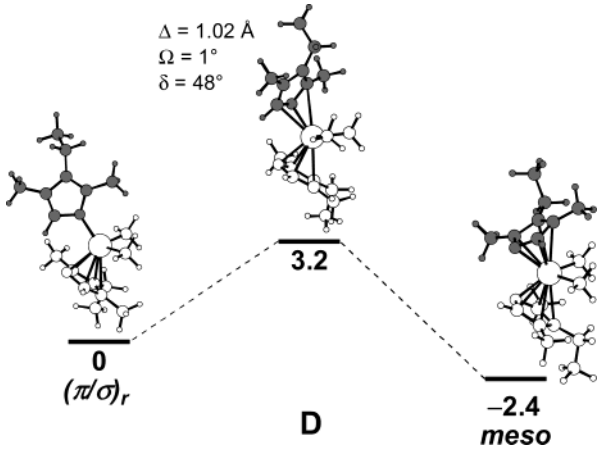

Figure 5. Energy profile (B3LYP) for the simultaneous slippage and rotation of the σ-dmep ligand from $(\pi/\sigma)_r$ to the *meso* form of $[Zr(\pi\text{-dmep})_2(CH_3)_2]$ (step D). The relative energies (bold, kcal mol^{-1}) and the coordination parameters of slipping and rotating dmep ligand (shaded) in the transition state are presented.

by the coordination parameters of Figure 5. Similarly to what happened with the first mechanism, the rate-limiting step corresponds to the slippage of the first dmep ligand from a π to a σ coordination (step A), since the slippage associated with the second step (D) starts from the less stable isomer, the π/σ species, and, thus, has a lower activation energy (3.2 kcal mol^{-1}).

The third and last mechanism of Scheme 6 is closely related to the first one, as it starts with the independent rotation and slippage of one dmep ligand from the *rac* isomer of the π/π complex to $(\pi/\sigma)_m$. But, in this case the order of the first two steps is reversed. First the dmep ligand rotates while π coordinated, reaching a different conformer of the *rac* form (*rac*′) in step E, and, then, the same dmep ligand slips from a π to a σ coordination, yielding $(\pi/\sigma)_m$ in step F. The last step (C) is common to the first mechanism, being the slippage from a σ bonded to a π-dmep, yielding the final *meso* product. This is a mechanism in three steps, E+F+C, composed by a rotation of a π-dmep followed by two consecutive slippages and corresponding to a "diagonal" connection between the two energy profiles of Figure 3. The last two steps, F+C, can be viewed as a flip of the dmep over the Zr−N bond, starting from one species where the two β carbon atoms of the slipping ring are on one side of the molecule (in *rac*′) to another (in *meso*) where the two β carbons are on the opposite side. In the transition state of step E, the rotating dmep ligand remains π coordinated with parameters equivalent to all the π-dmep here discussed (Figure 6, top). The *rac*′ conformer, obtained after step E, is 1.7 kcal mol^{-1} less stable than the original *rac* form, due to an increased interligand repulsion, making it closer, in stability terms, to the π/σ isomers than to any of the π/π complexes. However, the coordination geometry of the two dmep ligands in *rac*′ is essentially similar to all π-dmep reported here (Δ = 0.25/0.27 Å; Ω = 1/2°, δ = 80°). The coordination geometry of the slipping dmep in the transition state of step F is equivalent to what has been found in all the slippage steps (Figure 6, bottom). However, there is an important difference between step F and all the other slippage steps. Given the relative conformation of the two dmep ligands, in F the two β carbons of the slipping dmep are brought to the vicinity of the π-coordinated dmep. As a consequence, the coordination geometry of the π-dmep in the transition state adjusts in order to minimize this effect, being the more distorted (although flat: Ω = 1°) of all the first slippage transition states (A, C, D, and F). Nevertheless, it can still be called a slipped η^5-dmep, with Δ = 0.32 Å and δ = 78°. The activation energy associated with step E (3.5 kcal mol^{-1}) is readily accessible but considerably higher than the ones corresponding to the σ-dmep rotations ($\leq$1.9 kcal mol^{-1}), reflecting the dmep coordination mode (π) and the bulkiness of its substituents. The activation energy of step F (4.4 kcal mol^{-1}) fits in the values obtained for the slippage of the first dmep ligand, taking into account that the reactant (*rac*′) is 1.7 kcal mol^{-1} less stable than the original *rac* form. Step F is, thus, the rate-limiting step for this mechanism.

A last possibility for the interconversion between the *rac* and the *meso* forms of $[Zr(\pi\text{-dmep})_2(CH_3)_2]$, not considered in Scheme 6, involves the rotation of one dmep ligand of the σ/σ species. In this case, the mechanism has five steps: the first two are the consecutive slippage of each dmep in the *rac* form, leading to $(\sigma/\sigma)_r$, that is, the process depicted in the top energy profile of Figure 3 and discussed previously. A third step (G) converts $(\sigma/\sigma)_r$ in $(\sigma/\sigma)_m$ by means of the rotation of one dmep and makes the linkage between the two energy profiles of Figure 3. The last two steps correspond to the successive slippage of dmep from $(\sigma/\sigma)_m$ to the *meso* form of $[Zr(\pi\text{-dmep})_2(CH_3)_2]$ and to the energy profile depicted in the bottom of Figure 3. Step G is depicted in Figure 7, with the optimized geometries of the intervening species and the coordination parameters of the rotating dmep in the transition state. The rotation brings the dmep from a conformation, in $(\sigma/\sigma)_r$, where the α methyl group is over the ancillary ligands to another with the α methyl group opposite the Zr−CH_3 bonds, in $(\sigma/\sigma)_m$. The rotating dmep in the transition state has a typical σ coordination geometry, with coordination parameters similar to the ones calculated for all the σ-pyr′ reported here. Step G is a facile step with a low activation energy (1.9 kcal mol^{-1}), as expected for a rotation around a σ bond, and the rate-limiting step is the first π-dmep to σ-dmep slippage (step A).

Other mechanisms may be considered if one takes into account different conformations of the π- or σ-dmep ligands; however, since the rotation of these ligands in either coordination mode is easier than the slippage process, a major conclusion holds. In all the mechanisms the rate-limiting step corresponds to the first slippage of the dmep ligand from a π to a σ coordination mode. Namely, step F in the third mechanism, and step A in the others. The calculated activation energy for the *rac*/*meso* isomerization (4.4 kcal mol^{-1} for the third mechanism and 6.5 kcal mol^{-1} for the others) compares rather well with the experimental activation enthalpy (7.2 kcal mol^{-1}) estimated by a band coalescence method based on variable-temperature ^{1}H NMR results.[17] These numbers corroborate the observation of room-temperature fluxionality, not only in the dmep complexes here studied but also on the related $[Zr(\pi\text{-}PC_4PhMe_2H)_2Cl_2]$.[12,13] In simple terms, a crude analysis of the

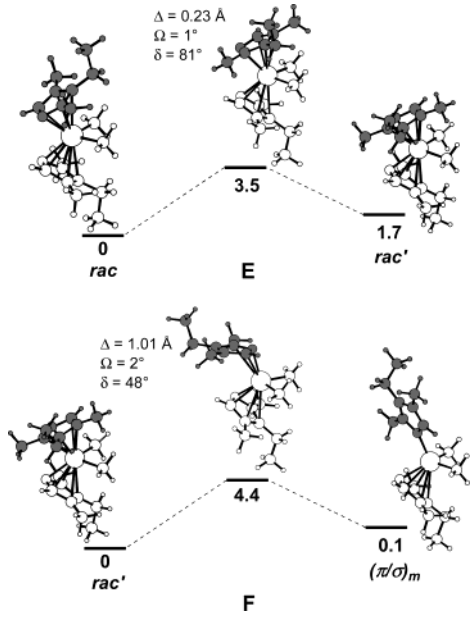

Figure 6. Energy profiles (B3LYP) for the rotation of one π-dmep ligand from *rac* to *rac*′ (step E, top) and for the $\pi-\sigma$ slippage of the same ligand from *rac*′ to $(\pi/\sigma)_m$ (step F, bottom). The relative energies (bold, kcal mol^{-1}) and the coordination parameters of slipping or rotating dmep ligand (shaded) in the transition states are presented.

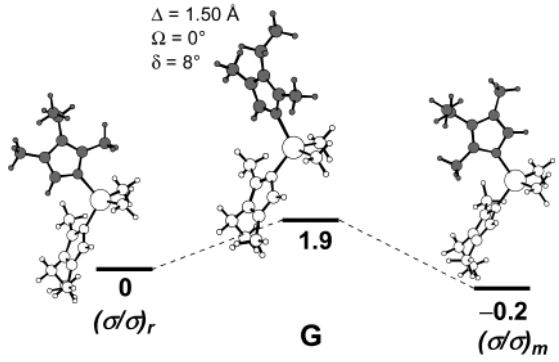

Figure 7. Energy profile (B3LYP) for the rotation of one σ-dmep ligand from $(\sigma/\sigma)_r$ to $(\sigma/\sigma)_m$ (step G). The relative energies (bold, kcal mol^{-1}) and the coordination parameters of the rotating dmep ligand (shaded) in the transition state are presented.

calculated activation energies indicates that the preferred mechanism for the *rac*/*meso* isomerization is the third one (E+F+C) corresponding to a rotation of one π-dmep, first, and then to two consecutive slippages. However, the similarity between the activation energies associated with the different mechanisms studied does not allow the attribution of a clear preference of one over the others, and, in addition, the low values obtained suggest that competition between all of them should be occurring in solution, even at room temperature.

Conclusions

From the slippage of a pyr′ from a π to a σ coordination mode results an electronically poorer metal center, and this process is, normally, associated with a destabilization of the complex. However, this destabilization is partially compensated by the changes in the nature of the Zr−N bond, much stronger in a σ-pyr′ coordination than in π-pyr′. For π-pyr′, the bonding geometry of the pyrrolyl ligand to the metal corresponds to a slightly distorted η^5 coordination with the nitrogen closer to the metal, while in a σ-pyr′ the metal−pyr′ bond is essentially a Zr−N σ interaction based on the nitrogen lone pair. Stereochemical effects play an important role in the balance for the relative stability of the two coordination modes. For example, substituents in the pyr′ α carbons disfavor the σ coordination and the $\pi-\sigma$ interconvertion.

Both in the case of monopyrrolyl complexes, [Zr(pyr′)L_3] and in the case of bispyrrolyl species, [Zr(pyr′)$_2L_2$], the interconversion between the two coordination modes of the pyrrolyl rings is, in fact, a slippage, since no significant folding of the NC_4 ring is observed along the entire process. In the corresponding transition state, the slipping ligand has a coordination geometry intermediate between the π and the σ modes: a flat η^3 coordination based on one strong Zr−N bond and two weak interactions between the metal and the two α carbon atoms of the ring.

Activation energies inferior to 10 kcal mol^{-1} were obtained for the slippage process of the different complexes, suggesting that, in most cases, a fluxional process involving the two coordination modes of the pyrrolyl ligand may occur in solution, even at room temperature. Thus, some caution has to be taken in the attribution of the coordination geometry of pyrrolyl ligands, based on solution experimental data, such as NMR chemical shifts.

The isomerization between the *rac* and the *meso* forms of [Zr(π-$NC_4Me_2EtH)_2(CH_3)_2$] proceeds via consecutive slippage and rotation of the asymmetric pyrrolyl ligand, but the rate-determining step is always the first slippage from a π to a σ coordination of that ligand. The low value obtained for the activation energy (E_a < 7 kcal mol^{-1}) corroborates the experimental observation of a fluxional process in solution, at room temperature.

Computational Details

All calculations were performed using the Gaussian 98 software package[32] and the B3LYP hybrid functional. That functional includes a mixture of Hartree−Fock[18] exchange with DFT[19] exchange−correlation, given by Becke's three-parameter functional[33] with the Lee, Yang, and Parr correlation functional, which includes both local and nonlocal terms.[34,35] The LanL2DZ basis set[36] augmented with an f-polarization function[37] was used for Zr, and a standard 6-31G(d,p)[38] for the remaining elements. Transition state optimizations were performed with the synchronous transit-guided quasi-Newton method (STQN) developed by Schlegel et al.[39] Frequency

(32) Frisch, M. J.; Trucks, G. W.; Schlegel, H. B.; Scuseria, G. E.; Robb, M. A.; Cheeseman, J. R.; Zakrzewski, V. G.; Montgomery, J. A., Jr.; Stratmann, R. E.; Burant, J. C.; Dapprich, S.; Millam, J. M.; Daniels, A. D.; Kudin, K. N.; Strain, M. C.; Farkas, O.; Tomasi, J.; Barone, V.; Cossi, M.; Cammi, R.; Mennucci, B.; Pomelli, C.; Adamo, C.; Clifford, S.; Ochterski, J.; Petersson, G. A.; Ayala, P. Y.; Cui, Q.; Morokuma, K.; Malick, D. K.; Rabuck, A. D.; Raghavachari, K.; Foresman, J. B.; Cioslowski, J.; Ortiz, J. V.; Stefanov, B. B.; Liu, G.; Liashenko, A.; Piskorz, P.; Komaromi, I.; Gomperts, R.; Martin, R. L.; Fox, D. J.; Keith, T.; Al-Laham, M. A.; Peng, C. Y.; Nanayakkara, A.; Gonzalez, C.; Challacombe, M.; Gill, P. M. W.; Johnson, B. G.; Chen, W.; Wong, M. W.; Andres, J. L.; Head-Gordon, M.; Replogle, E. S.; Pople, J. A. *Gaussian 98*, revision A.7; Gaussian, Inc.: Pittsburgh, PA, 1998.

(33) Becke, A. D.; J. *Chem. Phys.* **1993**, *98*, 5648.

(34) Miehlich, B.; Savin, A.; Stoll, H.; Preuss, H. *Chem. Phys. Lett.* **1989**, *157*, 200.

(35) Lee, C.; Yang, W.; Parr, G. *Phys. Rev. B* **1988**, *37*, 785.

calculations were performed to confirm the nature of the stationary points, yielding one imaginary frequency for the transition states and none for the minima. Each transition state was further confirmed by following its vibrational mode downhill on both sides and obtaining the minima presented on the energy profiles. All geometries were optimized without symmetry constraints, and the energies were zero-point corrected. A natural population analysis (NPA)[27] and the resulting Wiberg indices[26] were used for a detailed study of the electronic structure and bonding of the optimized species. NMR shielding tensors were calculated using the gauge-independent atomic orbital method (GIAO)[28] at the Hartree−Fock level using the same basis set for Zr and a 6-311+G(2d,p)[40] for the remaining elements.

The extended Hückel calculations[20,21] were done with the CACAO program,[41] and modified H_{ij} values were used.[42] The basis set for the metal atom consisted of *n*s, *n*p, and (*n*−1)d orbitals. The s and p orbitals were described by single Slater-type wave functions, and the d orbitals were taken as contracted linear combinations of two Slater-type wave functions. Only s and p orbitals were considered for Cl. The parameters used for Zr were the following (H_{ii} (eV), ζ): 5s −9.870, 1.817; 5p −6.760, 1.776; 4d −11.180, 3.835, 1.505 (ζ_2), 0. 6224 (C_1), 0.5782 (C_2). Standard parameters were used for other atoms. Calculations were performed on a [Zr(pyr)Cl_3] model complex based on the optimized geometry, with idealized maximum symmetry and the following distances (Å): Z−C(π-pyr) 2.25, W−N 2.25, Zr−Cl 2.35; and angle: X-Zr−Cl 115° (X is the pyrrolyl ring centroid).

Acknowledgment. A.P.F. acknowledges FCT for the PRAXIS XXI/BD/13348/97 scholarship.

Supporting Information Available: Tables of atomic coordinates (S1 to S43) and figures (S1 to S43) with the structure and relevant electronic and geometrical parameters, for all the optimized species. This material is available free of charge via the Internet at http://pubs.acs.org.

OM034029Y

(36) (a) Dunning, T. H., Jr.; Hay, P. J. *Modern Theoretical Chemistry*; Schaefer, H. F., III, Ed.; Plenum: New York, 1976; Vol. 3, p 1. (b) Hay, P. J.; Wadt, W. R. *J. Chem. Phys.* **1985**, *82*, 270. (c) Wadt, W. R.; Hay, P. J. *J. Chem. Phys.* **1985**, *82*, 284. (d) Hay, P. J.; Wadt, W. R. *J. Chem. Phys.* **1985**, *82*, 2299.

(37) Ehlers, A. W.; Böhme, M.; Dapprich, S.; Gobbi, A.; Höllwarth, A.; Jonas, V.; Köhler, K. F.; Stegmann, R.; Veldkamp A.; Frenking, G. *Chem. Phys. Lett.* **1993**, *208*, 111.

(38) Ditchfield, R.; Hehre W. J.; Pople, J. A. *J. Chem. Phys.* **1971**, *54*, 724. (b) Hehre, W. J.; Ditchfield R.; Pople, J. A. *J. Chem. Phys.* **1972**, *56*, 2257. (c) Hariharan, P. C.; Pople, J. A. *Mol. Phys.* **1974**, *27*, 209. (d) Gordon, M. S. *Chem. Phys. Lett.* **1980**, *76*, 163. (e) Hariharan, P. C.; Pople, J. A. *Theor. Chim. Acta* **1973**, *28*, 213.

(39) Peng, C.; Ayala, P. Y.; Schlegel, H. B.; Frisch, M. J. *J. Comput. Chem.* **1996**, *17*, 49. (b) Peng, C.; Schlegel, H. B. *Isr. J. Chem.* **1994**, *33*, 449.

(40) (a) McClean, A. D.; Chandler, G. S. *J. Chem. Phys.* **1980**, *72*, 5639. (b) Krishnan, R.; Binkley, J. S.; Seeger, R.; Pople, J. A. *J. Chem. Phys.* **1980**, *72*, 650. (c) Wachters, A. J. H. *J. Chem. Phys.* **1970**, *52*, 1033. (d) Hay, P. J. *J. Chem. Phys.* **1977**, *66*, 4377. (e) Raghavachari, K.; Trucks, G. W. *J. Chem. Phys.* **1989**, *91*, 1062. (f) Binning, R. C.; Curtiss, L. A. *J. Comput. Chem.* **1995**, *103*, 6104. (g) McGrath, M. P.; Radom, L. *J. Chem. Phys.* **1991**, *94*, 511.

(41) Mealli, C.; Proserpio, D. M. *J. Chem. Educ.* **1990**, *67*, 39.

(42) Ammeter, J. H.; Bürgi, H.-J.; Thibeault, J. C.; Hoffmann, R. *J. Am. Chem. Soc.* **1978**, *100*, 3686.